Evolution of coherence during ramps across the Mott-insulator–superfluid phase boundary

Yariv Yanay
Department of Physics, McGill University, Montreal, Canada H3A 2T8

Erich J. Mueller
Laboratory of Atomic and Solid State Physics, Cornell University, Ithaca New York 14850, USA

(Received 12 August 2015; revised manuscript received 17 December 2015; published 25 January 2016)

We calculate how correlations in a Bose lattice gas grow during a finite-speed ramp from the Mott to the superfluid regime. We use an interacting doublon-holon model, applying a mean-field approach for implementing hard-core constraints between these degrees of freedom. Our solutions are valid in any dimension and agree with experimental results and with density matrix renormalization group calculations in one dimension. We find that the final energy density of the system drops quickly with increased ramp time for ramps shorter than one hopping time, $J\tau_{\text{ramp}} \lesssim 1$. For longer ramps, the final energy density depends only weakly on ramp speed. We calculate the effects of inelastic light scattering during such ramps.

DOI: 10.1103/PhysRevA.93.013622

I. INTRODUCTION

The dynamics of systems driven through a phase transition are a source of rich physics [1]. The phenomenology is particularly interesting in zero-temperature systems driven through a quantum phase transition [2,3]. In recent years, breakthrough experimental techniques in atomic physics have given us a direct probe of such transitions [4–8]. In particular, a recent experiment [9] has probed the transition of a bosonic lattice system driven from a Mott-insulator state into the superfluid regime. The Bose–Hubbard model [10], which describes the physics of such experiments, is one of the fundamental models of many-body quantum mechanics, but the dynamics of its phase transition is not entirely understood. In this paper, we attempt to provide insight into this transition by introducing a novel mean-field theory, building on commonly used doublon-holon models [11]. We calculate how correlations develop during a lattice ramp through the phase transition.

The phase diagram of bosonic lattice systems has been explored thoroughly [10,12–15]. In the strongly interacting regime, at commensurate filling, lattice bosons form an incompressible Mott insulator. Conversely, for weak interactions the ground state is a superfluid Bose–Einstein condensate with long-range order. When the system begins in a Mott-insulator state and interactions are turned off, correlations grow as quasiparticles propagate across the system [16,17].

The Mott and superfluid phases can be approximated by distinct mean-field quasiparticle models. The excitations in the superfluid phase are well described by Bogoliubov quasiparticles made up of superpositions of particles and holes [18]. In the Mott-insulator regime, on-site number fluctuations are small and the occupation of each site can be truncated to a small number of possibilities [11]: the "doublon-holon" model. At strong coupling, doublons and holons can be approximated as noninteracting bosons. These two descriptions are incompatible, making it a challenge to model the dynamics across the phase boundary.

Previous work has produced a partial understanding of this transition [19,20]. Product-state methods such as the Gutzwiller ansatz cannot calculate correlations [21,22]. Other approaches have included calculations on small lattices [23], field theory calculations for large particle density [24–27], and various numerical techniques, which work well in one dimension but are otherwise more limited [28–30]. There has also been significant work on sudden quenches [31,32]. Approaches based on the Schwinger–Keldysh technique, which also produce equations of motion for relevant observables, have a long history in other fields [33]. More recently such approaches have been used to explore the phase diagram and order-parameter behavior in the Bose–Hubbard model [34,35].

Here, we provide an analytical model that is particularly suitable for the small mean occupation numbers common in atomic experiments, provides access to coherence data, and is applicable in any number of dimensions. We are able to see the growth of coherence as interactions are turned off, and how the rate at which they are turned off affects the correlations and final energy density of the system. We also model the effects of decoherence on such experiments, providing insights into the tradeoffs of experimental systems.

II. MODEL

The physics of atoms trapped in an optical lattice is well approximated by the Bose–Hubbard model [13], defined by the Hamiltonian

$$\hat{H}_{\text{BH}} = -J\sum_{\langle i,j\rangle}(\hat{a}_i^\dagger \hat{a}_j + \hat{a}_j^\dagger \hat{a}_i) + \frac{1}{2}[U]\sum_i \hat{n}_i(\hat{n}_i - 1). \quad (1)$$

Here $\hat{a}_i$ ($\hat{a}_i^\dagger$) is the annihilation (creation) operator for a boson on site i, while $\hat{n}_i = \hat{a}_i^\dagger \hat{a}_i$ is the number-density operator at site i. The sums are over nearest-neighbor pairs $\langle i,j\rangle$ and over all sites i. The hopping energy J and interaction energy U are parameters of the model.

We perform our calculation within an approximation called the doublon-holon model. We restrict the state of each site i to the subspace of occupations $|i\rangle \in \{|\bar{n}+1\rangle, |\bar{n}\rangle, |\bar{n}-1\rangle\}$, where $\bar{n}$ is the median number of particles per site. The system can then be thought of in terms of a mean-occupation background and hard-core quasiparticle excitations of "holons" (an $\bar{n}-1$ occupation) and "doublons" ($\bar{n}+1$ occupation). The annihilation operators at site i for these quasiparticles are defined by $\hat{d}_i|\bar{n}\rangle_i = \hat{d}_i|\bar{n}-1\rangle_i = \hat{h}_i|\bar{n}+1\rangle_i = \hat{h}_i|\bar{n}\rangle_i = 0$, $\hat{d}_i|\bar{n}+1\rangle_i = \hat{h}_i|\bar{n}-1\rangle_i = |\bar{n}\rangle_i$.

Under this approximation, the Hamiltonian is

$$\hat{H} = \sum_k \left[\frac{1}{2}[U] + J\sqrt{\bar{n}^2 + \frac{1}{4}\varepsilon_k}\right](\hat{d}_k^\dagger \hat{d}_k + \hat{h}_k^\dagger \hat{h}_k) + \frac{1}{2}[J]\varepsilon_k(\hat{d}_k^\dagger \hat{d}_k - \hat{h}_k^\dagger \hat{h}_k) + J\tilde{n}\varepsilon_k(\hat{d}_k\hat{h}_{-k} + \hat{h}_{-k}^\dagger \hat{d}_k^\dagger). \quad (2)$$

Here, $\hat{d}_k = \frac{1}{\sqrt{N_s}}\sum_i e^{i\boldsymbol{k}\cdot\boldsymbol{r}_i}\hat{d}_i$, summing over all sites i, and similar for $\hat{h}_k$, while $\varepsilon_k = -2\sum_\Delta \cos(\boldsymbol{k}\cdot\boldsymbol{\Delta})$, summing over lattice basis vectors, $\boldsymbol{\Delta} = \Delta\hat{x}, \Delta\hat{y}, \Delta\hat{z}$ in three dimensions, or a subset of those in lower dimensions. These represent a cubic lattice with lattice constant Δ. U and J are the interaction and hopping strength, respectively, and $\tilde{n} = \sqrt{\bar{n}(\bar{n}+1)}$. N_s is the number of sites in the lattice.

The doublon-holon model is an approximation for the single-band Bose–Hubbard model [10,36]. It is most accurate in the low-temperature, strongly interacting limit, because the energy of a state increases quadratically with the deviation from the mean particle number. However, for low occupation numbers $\bar{n}$, it can be a good approximation in the weakly interacting limit as well. In a noninteracting superfluid gas with $\bar{n} = 1$, the probability of finding more than two particles on a given site is less than 10%. We do all our calculations in this regime, taking, $\langle \hat{n}_i\rangle = \bar{n} + \langle \hat{d}_i^\dagger \hat{d}_i\rangle - \langle \hat{h}_i^\dagger \hat{h}_i\rangle = \bar{n} = 1$.

We calculate the time evolution of the two-point correlation functions, $\langle \hat{d}_k^\dagger \hat{d}_k\rangle \approx \langle \hat{h}_k^\dagger \hat{h}_k\rangle$ and $\langle \hat{d}_k \hat{h}_{-k}\rangle$, by using the Heisenberg equation, $\frac{d}{dt}\langle \hat{X}\rangle = i[\hat{H},\hat{X}]$. The hard-core constraints for $\hat{d}_i, \hat{h}_i$ imply nontrivial commutation relations, and the resulting equations of motion involve four-point correlation functions such as

$$C_{k,p,q} = \langle \hat{d}_p^\dagger \hat{h}_{-p-q}^\dagger \hat{h}_{-k-q} \hat{d}_k\rangle. \quad (3)$$

We can characterize $C_{k,p,q}$ by writing it in the form

$$C_{k,p,q} = \delta_{p,k}\langle \hat{h}_{-k-q}^\dagger \hat{h}_{-k-q}\rangle\langle \hat{d}_k^\dagger \hat{d}_k\rangle + \delta_{q,0}\langle \hat{d}_p^\dagger \hat{h}_{-p}^\dagger\rangle\langle \hat{h}_{-k}\hat{d}_k\rangle - \frac{\alpha_{k,p,q}}{N_s}\langle \hat{d}_k^\dagger \hat{d}_k\rangle. \quad (4)$$

This equation defines the function $\alpha_{p,k,q}$. We make a mean-field approximation, taking $\alpha_{p,k,q} \approx \frac{1}{n_d}\langle \hat{h}_{-p-q}^\dagger \hat{h}_{-p-q}\rangle\langle \hat{d}_p^\dagger \hat{d}_p\rangle$, where $n^d = \frac{1}{N_s}\sum_k \langle \hat{d}_k^\dagger \hat{d}_k\rangle$ is the doublon density. This approximation enforces the hard-core constraint $\sum_k C_{k,p,q} = 0$ and becomes exact in the deep Mott regime. We make similar approximation for the other four-point correlation functions, as detailed in Appendix. We arrive at a closed set of nonlinear coupled differential equations that we numerically integrate to find all quasiparticle two-point correlation functions at any time. From these we can easily extract the correlation functions for real particles, $\langle \hat{a}_i^\dagger \hat{a}_j\rangle$ and $\langle \hat{a}_k^\dagger \hat{a}_k\rangle$.

III. EQUILIBRIUM STATE

We find the equilibrium state under this model by minimizing the expectation value $\langle \hat{H}\rangle$ of the Hamiltonian of Eq. (2) while requiring the equations of motions (A17) to vanish.

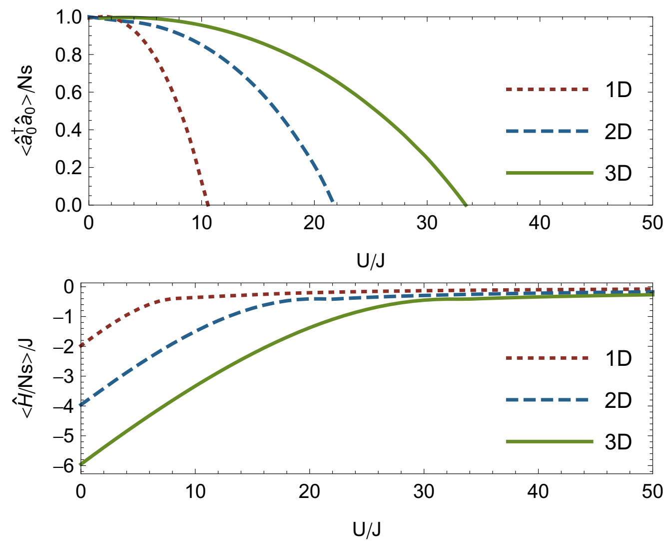

FIG. 1. Equilibrium properties of the hard-core doublon-holon model discussed in the text for a cubic lattice with mean filling $\bar{n} = 1$. Shown as a function of the interaction strength U/J, top: the equilibrium condensate fraction, bottom: the average energy per particle in the ground state.

We show the equilibrium properties of the model as we vary U/J in Fig. 1. The superfluid order parameter is the condensate density, $\frac{1}{N_s}\langle \hat{a}_k^\dagger \hat{a}_k\rangle_{k=0}$. We find a phase transition at a critical value of $U_c/J = 10.4$, 21.8, 33.4 in one, two and three dimensions, respectively. These are similar to the standard mean-field values of $U_c/J = 11.6$, 23.2, 34.8 [12,37] and somewhat higher than numerically calculated values $U_c/J = 3.6$, 16.9, 29.3 [38–43]. We also plot the behavior of the ground-state energy density, $\frac{1}{N_s}\langle \hat{H}\rangle$. At $U = 0$, the Bose–Hubbard model in D dimensions has a ground-state energy density of $-2DJ$. In our model the energy density reaches a small but finite value above these values.

IV. INTERACTION RAMPS

We use the model above to explore the behavior of a gas subject to a nonadiabatic ramp of the interaction through the phase transition. We perform an interaction ramp of the form

$$U = U_i(U_f/U_i)^{t/\tau_r}, \quad (5)$$

where the ground state of the system is a Mott insulator for $U = U_i$ and a superfluid for $U = U_f$. The timescale τ_r sets the speed of the ramp. This form approximates the relation U/J in an optical-lattice experiment if the scattering length is fixed and the lattice depth is ramped down [13].

We initialize the system in the ground state at the initial lattice depth, in the Mott regime, and perform a finite-element time integration of the evolution equations as the interaction strength is reduced. We calculate the momentum-space density throughout this evolution for various values of τ_r. Figure 2 shows the behavior for a typical ramp, with $J\tau_r = 2$. We have full access to all two-point observables at any time along the ramp.

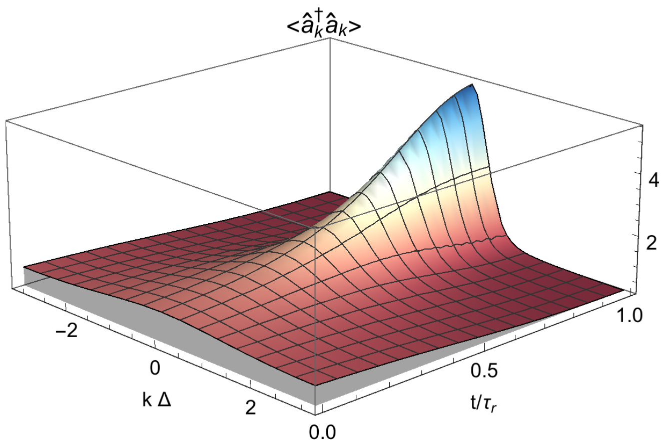

FIG. 2. Evolution of the momentum-density distribution function $\langle \hat{a}_k^\dagger \hat{a}_k \rangle$ as the interaction strength is slowly ramped down, $U = U_i(U_f/U_i)^{t/\tau_r}$ in a one-dimensional lattice. Here $U_i = 47J$, $U_f = 2J$, $J\tau_r = 2$.

We first characterize the behavior of the system at the end of the ramp. We define an effective correlation length ξ by comparing correlations in the system to the form $\langle \hat{a}_i^\dagger \hat{a}_j \rangle = \bar{n} e^{-|\mathbf{r}_j - \mathbf{r}_i|/\xi}$. We calculate ξ by fitting to the width of the momentum distribution, as defined by the first moment, yielding

$$\frac{\xi}{\Delta} = -1/\ln\left[\frac{1}{N_s}\sum_k \frac{\varepsilon_k}{\varepsilon_0}\langle \hat{a}_k^\dagger \hat{a}_k \rangle\right]. \quad (6)$$

Although it is infinite for an equilibrium superfluid system, ξ remains finite at any finite time for a system that is not initially superfluid [16].

Figure 3 shows the effective correlation length at the end of the ramp for varying ramp times. Our calculation agrees with the experimental results and, in one dimension, the DMRG results of Ref. [9]. In one dimension, we also compare our calculation to the results of an exact diagonalization of the Hamiltonian of Eq. (2) on a nonperiodic lattice with $N_s = 11$. The results agree well with our approximate calculation.

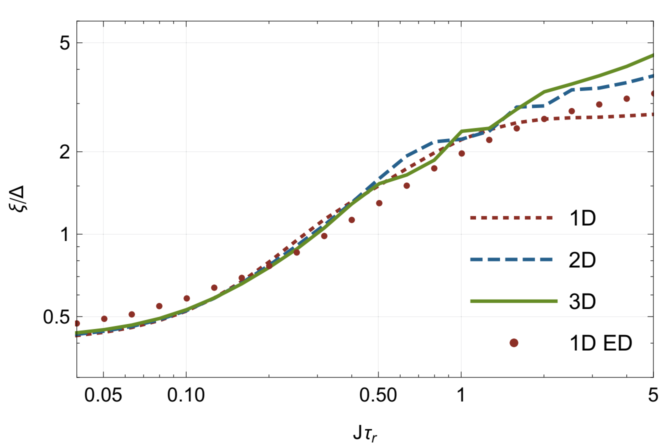

FIG. 3. Effective correlation length ξ [see Eq. (6)], normalized by the lattice constant Δ, at the end of a ramp of the interaction strength of the form $U = U_i(U_f/U_u)^{t/\tau_r}$. Here $U_i = 47J$, $U_f = 2J$. The red dots are the result of an exact diagonalization calculation for an 11-site one-dimensional lattice.

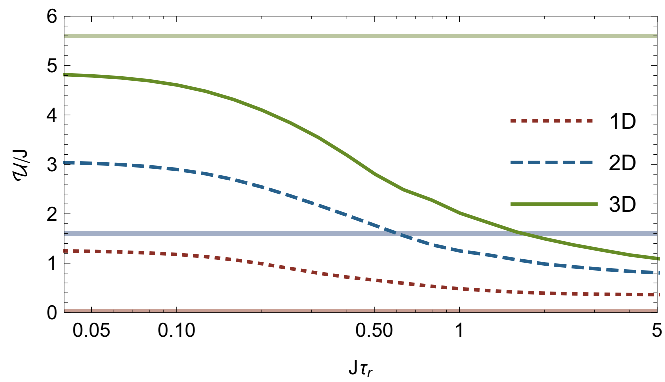

FIG. 4. The energy density $\mathcal{U}$ following an interaction ramp of the form $U = U_i(U_f/U_i)^{t/\tau_r}$. Here $U_i = 47J$, $U_f = 2J$. Horizontal lines show the energy density, $\mathcal{U}_c/J = 0$, 2.1, 5.1, at the superfluid critical temperature $T_c/J = 0$, 1.7, 5.9, for $U = U_f = 2J$, in one, two and three dimensions, respectively [41,42].

V. FINAL ENERGY DENSITY

After the ramp has ended, the system continues to evolve, and the correlation length continues to grow. However, the energy of the system is now conserved. At long times after the ramp we expect the state of the system to resemble a thermal state at a temperature determined by the energy density $\mathcal{U} = \frac{1}{N_s}[\langle \hat{H} \rangle - \langle \hat{H} \rangle_{\text{g.s.}}]$, where $\langle \hat{H} \rangle_{\text{g.s.}}$ is the energy of the ground state of the system with its final parameters.

We plot $\mathcal{U}$ as a function of the ramp time τ_r in Fig. 4. For ramp times much shorter than the hopping timescale, $J\tau_r \lesssim 0.2$, the final energy density varies slowly with τ_r. Such ramps are indistinguishable from instantaneous quenches, and the final state of the system, if allowed to equilibrate, would be similar for any τ_r in this regime. For $J\tau_r \gtrsim 0.2$, the system's energy depends more strongly on the length of the ramp.

Figure 4 also shows the critical energy density $\mathcal{U}_c$ corresponding to the energy density of of a Bose lattice gas with $U = U_f$ at the critical temperature of the superfluid–normal-gas phase transition [41,42]. We expect a gas with $\mathcal{U} > \mathcal{U}_c$ to equilibrate to a normal-gas state with finite correlation length ξ, while a gas at $\mathcal{U} < \mathcal{U}_c$ would equilibrate to a superfluid state with long-range order. In two dimensions, we expect short ramps, $J\tau_r \lesssim 0.6$, to lead to a normal state, while longer ramps lead to a superfluid gas. In three dimensions, the energy density is always below $\mathcal{U}_c$, even for an instantaneous quench. In one dimension there is no condensed phase.

VI. DECOHERENCE

In an ideal, closed, quantum system, all evolution is unitary. The final energy of the system rises monotonically with the rate of the ramp in such systems. Conversely, any real system suffers from heating, atom loss, and other impacts from the environment. As a result, experimental dynamic systems always face a competition between the system's reaction time and external processes.

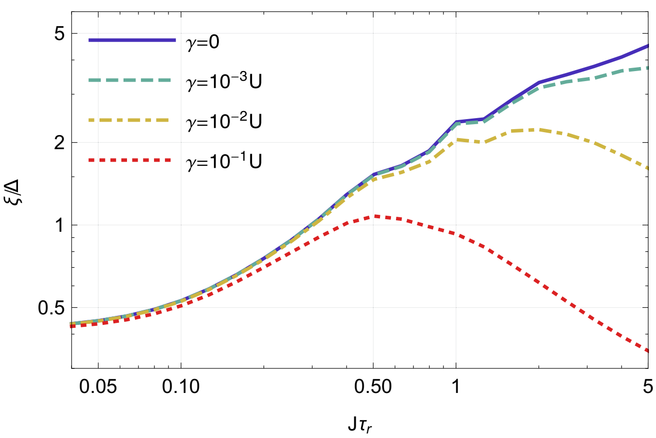

FIG. 5. Effective correlation length ξ, at the end of a ramp of the interaction strength, in a system coupled to the environment in the form shown in Eq. (7). Here $U_f = 47J$, $U_i = 2J$, in a three-dimensional cubic lattice. In an optical lattice setup, the rate of inelastic light scattering events changes with lattice depth similarly to the interaction strength [13,49]. In atomic experiments a typical value is $\gamma \sim 10^{-2}U$ [44].

The physics of such decoherence has been explored in detail [44–49]. Here, we return to a mechanism we previously used to describe the effect of density measurements by light scattering [50]. The same formalism describes inelastic light scattering, where an external photon scatters from a trapped atom. This is one of the major sources of decoherence in atomic experiments.

As in Ref. [50], we neglect out-of-band effects, which cause particle loss. We focus on in-band scattering, which would directly decrease the coherence of the remaining gas and reduce the correlation length measured above. In an ensemble description, this leads to a nonunitary evolution term of the form

$$\begin{aligned}\frac{d}{dt}\langle \hat{d}_k^\dagger \hat{d}_k\rangle &= -i\langle[\hat{d}_k^\dagger \hat{d}_k,\hat{H}]\rangle - \gamma(\langle \hat{d}_k^\dagger \hat{d}_k\rangle - n_d),\\ \frac{d}{dt}\langle \hat{d}_k \hat{h}_{-k}\rangle &= -i\langle[\hat{d}_k \hat{h}_{-k},\hat{H}]\rangle - \gamma\langle \hat{d}_k \hat{h}_{-k}\rangle,\end{aligned} \tag{7}$$

where γ is proportional to the frequency of light scattering per site.

We calculate the effect of this decoherence on the behavior of the correlation length ξ, as shown in Fig. 5. As expected, no effect is seen at timescales shorter than $1/\gamma$. At longer timescales, inelastic processes cause the correlation length to decay. The overall effect is similar to experimental observations in Ref. [9]. We thus find that the optimal ramp time depends on the interplay of adiabaticity and decoherence. For decoherence rates typical of atomic experiments, $\gamma \sim 10^{-2}U$, this optimal time is on the scale of $J\tau_r \sim 1$.

VII. OUTLOOK

The physics of ultracold atomic systems involves multiple energy scales. In driven experimental systems, these include the relaxation time of the system, the driving timescale, and the rate of decoherence imposed by interaction with the environment. Here, we quantified the effect of the quench rate in Bose–Hubbard systems crossing the phase boundary. We find that there are two regimes. For sweeps that are much shorter than the typical hopping time, $J\tau_r \lesssim 0.2$, the ramp time has no effect on the final state and the ramp is indistinguishable from an instantaneous quench. For longer ramps, the final energy density of the state and therefore its correlations at equilibrium depend on the length of the ramp. In two dimensions, shorter ramps lead to a normal gas state, while longer ramps lead to a superfluid state. We also demonstrated that inelastic light scattering can be quite destructive on longer timescales, underscoring the usefulness of shorter experimental runs.

ACKNOWLEDGMENTS

We acknowledge support from the ARO-MURI Nonequilibrium Many-Body Dynamics Grant No. 63834-PH-MUR.

APPENDIX: DETAILED DERIVATION OF MEAN-FIELD APPROXIMATION

1. Underlying Model

We perform our calculation within an approximate "doublon-holon" model. The state of each site i can be given in terms of a spinor in the allowed occupation states $|\bar{n}+1\rangle_i$, $|\bar{n}\rangle_i$, $|\bar{n}-1\rangle_i$ where $\bar{n}$ is the median number of particles per site. We define the quasiparticle annihilation operators, $\hat{d}_i = |\bar{n}\rangle\langle\bar{n}+1|_i$, $\hat{h}_i = |\bar{n}\rangle\langle\bar{n}-1|_i$.

Under this approximation, the Hamiltonian is

$$\begin{aligned}\hat{H} &= -J\sum_{\langle i,j\rangle}\left[\begin{array}{c}(\bar{n}+1)\hat{d}_i^\dagger\hat{d}_j + \bar{n}\hat{h}_i^\dagger\hat{h}_j\\ +\sqrt{\bar{n}(\bar{n}+1)}(\hat{d}_i\hat{h}_j + \hat{d}_j^\dagger\hat{h}_i^\dagger)\end{array} + \text{H.c.}\right]\\ &\quad + \frac{U}{2}\sum_i(\hat{d}_i^\dagger\hat{d}_i + \hat{h}_i^\dagger\hat{h}_i)\\ &= \sum_k\left[\begin{array}{c}\left(\tfrac{1}{2}U + J\sqrt{\tilde{n}^2+\tfrac{1}{4}}\varepsilon_k\right)(\hat{d}_k^\dagger\hat{d}_k + \hat{h}_k^\dagger\hat{h}_k)\\ +\tfrac{1}{2}J\varepsilon_k(\hat{d}_k^\dagger\hat{d}_k - \hat{h}_k^\dagger\hat{h}_k)\\ +J\tilde{n}\varepsilon_k(\hat{d}_k\hat{h}_{-k} + \hat{h}_{-k}^\dagger\hat{d}_k^\dagger)\end{array}\right].\end{aligned} \tag{A1}$$

Here,

$$\hat{d}_k = \frac{1}{\sqrt{N_s}}\sum_i e^{i\boldsymbol{k}\cdot\boldsymbol{r}_i}\hat{d}_i, \quad \hat{h}_k = \frac{1}{\sqrt{N_s}}\sum_i e^{i\boldsymbol{k}\cdot\boldsymbol{r}_i}\hat{h}_i, \tag{A2}$$

summing over all sites i, and

$$\varepsilon_k = -2\sum_\Delta \cos(\boldsymbol{k}\cdot\boldsymbol{\Delta}), \tag{A3}$$

summing over lattice basis vectors. We perform our calculation on a cubic lattice with lattice spacing Δ, $\boldsymbol{\Delta} = \Delta\hat{x},\Delta\hat{y},\Delta\hat{z}$ in three dimensions, or a subset of those in lower dimensions. U and J are the interaction and hopping strength, respectively, and $\tilde{n} = \sqrt{\bar{n}(\bar{n}+1)}$. N_s is the number of sites in the lattice.

We do all our calculations for a density of one particle per site, $\langle\hat{n}_i\rangle = \bar{n} + \langle\hat{d}_i^\dagger\hat{d}_i\rangle - \langle\hat{h}_i^\dagger\hat{h}_i\rangle = \bar{n} = 1$.

The hard-core constraints on the operators $\hat{d}$, $\hat{h}$ translate into nontrivial commutation relations:

$$[\hat{d}_k,\hat{d}_q^\dagger] = \delta_{k,q} - 2\hat{n}^d_{q-k} - \hat{n}^h_{q-k}, \quad [\hat{h}_k,\hat{h}_q^\dagger] = \delta_{k,q} - \hat{n}^d_{q-k} - 2\hat{n}^h_{q-k},$$
$$[\hat{d}_k^\dagger,\hat{h}_q] = \hat{\nu}_{q-k}, \quad [\hat{h}_k^\dagger,\hat{d}_q] = \hat{\nu}^\dagger_{k-q}, \quad [\hat{d}_k,\hat{d}_q] = [\hat{h}_k,\hat{h}_q] = [\hat{d}_k,\hat{h}_q] = 0, \tag{A4}$$

where we define the quasiparticle-density operators

$$\hat{n}^d_k = \frac{1}{N_s}\sum_i e^{-i\boldsymbol{k}\cdot r_i}\hat{d}_i^\dagger\hat{d}_i, \quad \hat{n}^h_k = \frac{1}{N_s}\sum_i e^{-i\boldsymbol{k}\cdot r_i}\hat{h}_i^\dagger\hat{h}_i, \quad \hat{\nu}^\dagger_k = \frac{1}{N_s}\sum_i e^{-i\boldsymbol{k}\cdot r_i}\hat{h}_i^\dagger\hat{d}_i. \tag{A5}$$

We write $\hat{n}_{d,h} \equiv \hat{n}_0^{d,h}$, the density of doublons and holons, respectively. In the Mott equilibrium limit, the operators in Eq. (A5) can be neglected and the quasiparticles can be treated as noninteracting bosons. This is not true in the superfluid regime.

2. Equations of Motion

Equations of motion can be derived from the Hamiltonian (A1) via the Heisenberg equation,

$$\frac{d}{dt}\langle\hat{X}\rangle = i[\hat{X},\hat{H}]. \tag{A6}$$

We focus on the two-point observables, $\langle\hat{d}_k^\dagger\hat{d}_k\rangle$, $\langle\hat{h}_k^\dagger\hat{h}_k\rangle$, $\langle\hat{d}_k\hat{h}_{-k}\rangle$. Their full equations of motion are given by

$$\frac{d}{dt}\langle\hat{d}_k^\dagger\hat{d}_k\rangle = iJ\tilde{n}\varepsilon_k(\langle\hat{d}_k\hat{h}_{-k}\rangle - \langle\hat{d}_k^\dagger\hat{h}^\dagger_{-k}\rangle) - iJ\tilde{n}\sum_q\varepsilon_q\left[\begin{matrix}\left(\sqrt{1+\frac{1}{4\tilde{n}^2}}+\frac{1}{2\tilde{n}}\right)\langle\hat{d}_q^\dagger(2\hat{n}^d_{k-q}+\hat{n}^h_{k-q})\hat{d}_k\rangle\\ +\left(\sqrt{1+\frac{1}{4\tilde{n}^2}}-\frac{1}{2\tilde{n}}\right)\langle\hat{h}^\dagger_{-q}\hat{\nu}_{-k-q}\hat{d}_k\rangle\\ +\langle(2\hat{n}^d_{k-q}+\hat{n}^h_{k-q})\hat{h}_{-q}\hat{d}_k\rangle + \langle\hat{\nu}_{-q-k}\hat{d}_q\hat{d}_k\rangle\end{matrix} - \text{H.c.}\right],$$

$$\frac{d}{dt}\langle\hat{h}^\dagger_{-k}\hat{h}_{-k}\rangle = iJ\tilde{n}\varepsilon_k(\langle\hat{d}_k\hat{h}_{-k}\rangle - \langle\hat{d}_k^\dagger\hat{h}^\dagger_{-k}\rangle) - iJ\tilde{n}\sum_q\varepsilon_q\left[\begin{matrix}\left(\sqrt{1+\frac{1}{4\tilde{n}^2}}-\frac{1}{2\tilde{n}}\right)\langle\hat{h}^\dagger_{-q}(2\hat{n}^h_{q-k}+\hat{n}^d_{q-k})\hat{h}_{-k}\rangle\\ +\left(\sqrt{1+\frac{1}{4\tilde{n}^2}}+\frac{1}{2\tilde{n}}\right)\langle\hat{d}_q^\dagger\hat{\nu}^\dagger_{-q-k}\hat{h}_{-k}\rangle\\ +\langle(2\hat{n}^h_{q-k}+\hat{n}^d_{q-k})\hat{d}_q\hat{h}_{-k}\rangle + \langle\hat{\nu}^\dagger_{-q-k}\hat{h}_{-q}\hat{h}_{-k}\rangle\end{matrix} - \text{H.c.}\right],$$

$$\frac{d}{dt}\langle\hat{d}_k\hat{h}_{-k}\rangle = -iU\langle\hat{d}_k\hat{h}_{-k}\rangle - iJ\tilde{n}\varepsilon_k(1-3n_d-3n_h) - iJ\tilde{n}\sum_q\varepsilon_q\left(\delta_{k,q}-\frac{1}{N_s}\right)\left[2\sqrt{1+\frac{1}{4\tilde{n}^2}}\langle\hat{d}_q\hat{h}_{-q}\rangle + \langle\hat{d}_q^\dagger\hat{d}_q\rangle + \langle\hat{h}^\dagger_{-q}\hat{h}_{-q}\rangle\right]$$
$$+iJ\tilde{n}\sum_q\varepsilon_q\left[\begin{matrix}\left(\sqrt{1+\frac{1}{4\tilde{n}^2}}+\frac{1}{2\tilde{n}}\right)\left(\langle\hat{h}_{-q}(2\hat{n}^d_{k-q}+\hat{n}^h_{k-q})\hat{d}_k\rangle + \langle\hat{d}_q\hat{\nu}_{-q-k}\hat{d}_k\rangle\right)\\ +\left(\sqrt{1+\frac{1}{4\tilde{n}^2}}-\frac{1}{2\tilde{n}}\right)\left(\langle\hat{d}_q(\hat{n}^d_{q-k}+2\hat{n}^h_{q-k})\hat{h}_{-k}\rangle + \langle\hat{h}_{-q}\hat{\nu}^\dagger_{-q-k}\hat{h}_{-k}\rangle\right)\\ +\langle\hat{h}^\dagger_{-q}(2\hat{n}^d_{q-k}+\hat{n}^h_{q-k})\hat{h}_{-k}\rangle + \langle\hat{d}_q^\dagger\hat{\nu}^\dagger_{-q-k}\hat{h}_{-k}\rangle\\ +\langle\hat{d}_q^\dagger(\hat{n}^d_{k-q}+2\hat{n}^h_{k-q})\hat{d}_k\rangle + \langle\hat{h}^\dagger_{-q}\hat{\nu}_{-q-k}\hat{d}_k\rangle\\ -(2\hat{n}^d_{q-k}+\hat{n}^h_{q-k})(\hat{n}^d_{k-q}+2\hat{n}^h_{k-q}) - \frac{1}{2}(\hat{\nu}^\dagger_{-q-k}\hat{\nu}_{-q-k}+\hat{\nu}_{-q-k}\hat{\nu}^\dagger_{-q-k})\end{matrix}\right]. \tag{A7}$$

Here H.c. stands for the Hermitian conjugate.

3. Hard-Core Coherent Approximation

To perform the time evolution, we must make approximations for the quartic terms, such as

$$\mathcal{C}^1_k = \sum_q\varepsilon_q\langle\hat{d}_q^\dagger\hat{n}^h_{k-q}\hat{d}_k\rangle \equiv \frac{1}{N_s}\sum_{p,q}\varepsilon_q C_{k,q,p}. \tag{A8}$$

Written out explicitly, we have

$$\mathcal{C}^1_k = \frac{1}{N_s}\sum_p\varepsilon_k\langle\hat{d}_k^\dagger\hat{h}^\dagger_{-k-p}\hat{h}_{-k-p}\hat{d}_k\rangle + \frac{1}{N_s}\sum_q\varepsilon_q\langle\hat{d}_q^\dagger\hat{h}^\dagger_{-q}\hat{h}_{-k}\hat{d}_k\rangle - \frac{1}{N_s}\varepsilon_k\langle\hat{d}_k^\dagger\hat{h}^\dagger_{-k}\hat{h}_{-k}\hat{d}_k\rangle + \frac{1}{N_s}\sum_{\substack{p,q\\ q\neq k,p\neq 0}}\varepsilon_q\langle\hat{d}_q^\dagger\hat{h}^\dagger_{-p-q}\hat{h}_{-k-q}\hat{d}_k\rangle. \tag{A9}$$

The first two sums on the right-hand side add up coherently, and we expect them to dominate. The third term is inversely proportional to the system size and is therefore negligible. For bosonic operators, one may expect the final summation term to add up incoherently, as in the Hartree–Fock–Bogoliubov approximation [18]. This suggests the form

$$\mathcal{C}_k^1 \approx \tilde{\mathcal{C}}_k^1 = \left(\frac{1}{N_s}\sum_p \langle \hat{h}^\dagger_{-k-p}\hat{h}_{-k-p}\rangle\right)\varepsilon_k\langle \hat{d}_k^\dagger \hat{d}_k\rangle + \left(\frac{1}{N_s}\sum_q \varepsilon_q\langle \hat{d}_q^\dagger \hat{h}^\dagger_{-q}\rangle\right)\langle \hat{h}_{-k}\hat{d}_k\rangle. \tag{A10}$$

This intuition fails in the hard-core case. This can be seen by summing over the momenta,

$$\sum_k \mathcal{C}_k^1 = \frac{1}{N_s}\sum_{p,q,k}\varepsilon_q\langle \hat{d}_q^\dagger \hat{h}^\dagger_{-p-q}\hat{h}_{-p-k}\hat{d}_k\rangle = \frac{1}{N_s}\sum_{p,q,i} e^{ipr_i}\varepsilon_q\langle \hat{d}_q^\dagger \hat{h}^\dagger_{-p-q}\hat{h}_i\hat{d}_i\rangle = 0, \quad \sum_k \tilde{\mathcal{C}}_k^1 = \langle \hat{n}_h\rangle\left(\sum_k \varepsilon_k\langle \hat{d}_k^\dagger \hat{d}_k\rangle\right) \neq 0. \tag{A11}$$

To account for the hard-core constraints, we expand

$$C^1_{k,p,q} = \langle \hat{d}_q^\dagger \hat{h}^\dagger_{-p-q}\hat{h}_{-p-k}\hat{d}_k\rangle \equiv \delta_{k,q}\langle \hat{h}^\dagger_{-p-q}\hat{h}_{-p-k}\rangle\langle \hat{d}_k^\dagger \hat{d}_k\rangle + \delta_{p,0}\langle \hat{d}_q^\dagger \hat{h}^\dagger_{-q}\rangle\langle \hat{h}_{-k}\hat{d}_k\rangle - \frac{\alpha_{k,p,q}}{N_s}\langle \hat{d}_k^\dagger \hat{d}_k\rangle. \tag{A12}$$

Formally, Eq. (A12) defines $\alpha_{k,p,q}$. We approximate this function with the hard-core constraint in mind as

$$\alpha_{k,p,q} \approx \frac{1}{\langle \hat{n}^d\rangle}\langle \hat{h}^\dagger_{-p-q}\hat{h}_{-p-q}\rangle\langle \hat{d}_q^\dagger \hat{d}_q\rangle, \tag{A13}$$

so that $\sum_k C^1_{k,p,q} = 0$.

We then find

$$\mathcal{C}_k^1 = \frac{1}{N_s}\sum_{p,q} C^1_{k,p,q} \approx \langle \hat{n}^h\rangle\left(\varepsilon_k - \varepsilon_0\frac{\xi_d}{n_d}\right)\langle \hat{d}_k^\dagger \hat{d}_k\rangle + \varepsilon_0\eta^*\langle \hat{d}_k\hat{h}_{-k}\rangle, \tag{A14}$$

where

$$n_d = \langle \hat{n}^d\rangle, \quad \xi_d = \frac{1}{N_s}\sum_k \frac{\varepsilon_k}{\varepsilon_0}\langle \hat{d}_k^\dagger \hat{d}_k\rangle, \quad \eta = \frac{1}{N_s}\sum_k \frac{\varepsilon_k}{\varepsilon_0}\langle \hat{d}_k\hat{h}_{-k}\rangle. \tag{A15}$$

We make similar approximations for the other terms:

$$\begin{aligned}
\langle \hat{d}_q^\dagger \hat{d}^\dagger_{p-q}\hat{d}_{p-k}\hat{d}_k\rangle &\approx \delta_{q,k}\langle \hat{d}^\dagger_{p-k}\hat{d}_{p-k}\rangle\langle \hat{d}_k^\dagger \hat{d}_k\rangle + \delta_{p-q,k}\langle \hat{d}_q^\dagger \hat{d}_q\rangle\langle \hat{d}_k^\dagger \hat{d}_k\rangle - \frac{2}{N_s}\frac{1}{n_d}\langle \hat{d}_q^\dagger \hat{d}_q\rangle\langle \hat{d}^\dagger_{p-q}\hat{d}_{p-q}\rangle\langle \hat{d}_k^\dagger \hat{d}_k\rangle,\\
\langle \hat{h}^\dagger_{-q}\hat{d}^\dagger_{p+q}\hat{h}_{p-k}\hat{d}_k\rangle &\approx \delta_{p,0}\langle \hat{h}^\dagger_{-q}\hat{d}_q^\dagger\rangle\langle \hat{d}_k\hat{h}_{-k}\rangle + \delta_{p+q,k}\langle \hat{h}^\dagger_{-q}\hat{h}_{-q}\rangle\langle \hat{d}_k^\dagger \hat{d}_k\rangle - \frac{1}{N_s}\frac{1}{n_d}\langle \hat{h}^\dagger_{-q}\hat{h}_q\rangle\langle \hat{d}^\dagger_{p+q}\hat{d}_{p+q}\rangle\langle \hat{d}_k^\dagger \hat{d}_k\rangle,\\
\langle \hat{h}_{-q}\hat{h}^\dagger_{-p-q}\hat{h}_{-p-k}\hat{d}_k\rangle &\approx \delta_{p,0}\langle \hat{h}_{-q}\hat{h}^\dagger_{-q}\rangle\langle \hat{d}_k\hat{h}_{-k}\rangle + \delta_{q,k}\langle \hat{h}^\dagger_{-p-k}\hat{h}_{-p-k}\rangle\langle \hat{d}_k\hat{h}_{-k}\rangle - \frac{1}{N_s}\frac{1}{n_d}\langle \hat{h}^\dagger_{-p-q}\hat{h}_{-p-q}\rangle\langle \hat{d}_q\hat{h}_{-q}\rangle\langle \hat{d}_k^\dagger \hat{d}_k\rangle,\\
\langle \hat{h}_{-q}\hat{d}^\dagger_{p-q}\hat{d}_{p-k}\hat{d}_k\rangle &\approx \delta_{q,k}\langle \hat{d}^\dagger_{p-k}\hat{d}_{p-k}\rangle\langle \hat{d}_k\hat{h}_{-k}\rangle + \delta_{p-q,k}\langle \hat{d}_q\hat{h}_{-q}\rangle\langle \hat{d}_k^\dagger \hat{d}_k\rangle - \frac{2}{N_s}\frac{1}{n_d}\langle \hat{d}_q\hat{h}_{-q}\rangle\langle \hat{d}^\dagger_{p-q}\hat{d}_{p-q}\rangle\langle \hat{d}_k^\dagger \hat{d}_k\rangle,\\
\langle \hat{d}_q\hat{d}^\dagger_{p+q}\hat{h}_{p-k}\hat{d}_k\rangle &\approx \delta_{p,0}\langle \hat{d}_q\hat{d}_q^\dagger\rangle\langle \hat{d}_k\hat{h}_{-k}\rangle + \delta_{p+q,k}\langle \hat{d}_q\hat{h}_{-q}\rangle\langle \hat{d}_k^\dagger \hat{d}_k\rangle - \frac{1}{N_s}\frac{1}{n_d}\langle \hat{d}_q\hat{h}_{-q}\rangle\langle \hat{d}^\dagger_{p+q}\hat{d}_{p+q}\rangle\langle \hat{d}_k^\dagger \hat{d}_k\rangle.
\end{aligned} \tag{A16}$$

Applying these approximations to Eq. (A7), we find

$$\begin{aligned}
\frac{d}{dt}\langle \hat{d}_k^\dagger \hat{d}_k\rangle &= iJ\tilde{n}\varepsilon_k(\langle \hat{d}_k\hat{h}_{-k}\rangle - \langle \hat{d}_k^\dagger \hat{h}^\dagger_{-k}\rangle) - iJ\tilde{n}\left[\begin{matrix} 3(\varepsilon_k n_d\langle \hat{d}_k\hat{h}_{-k}\rangle - \varepsilon_0\eta\langle \hat{d}_k^\dagger \hat{d}_k\rangle)\\ +2\varepsilon_0\big(\sqrt{1+\frac{1}{4\tilde{n}^2}}\eta^*\langle \hat{d}_k\hat{h}_{-k}\rangle + \xi_d\langle \hat{d}_k\hat{h}_{-k}\rangle\big)\end{matrix} - \text{H.c.}\right],\\
\frac{d}{dt}\langle \hat{d}_k\hat{h}_{-k}\rangle &= -iU\langle \hat{d}_k\hat{h}_{-k}\rangle - iJ\tilde{n}\varepsilon_k\big[1-6n_d+9\big(n_d^2-\xi_d^2\big)+6|\eta|^2\big] - 2iJ\tilde{n}\left[\sqrt{1+\frac{1}{4\tilde{n}^2}}(\langle \hat{d}_q\hat{h}_{-q}\rangle - \eta) + \langle \hat{d}_k^\dagger \hat{d}_k\rangle - \xi_d\right]\\
&\quad + 2iJ\tilde{n}\left[\begin{matrix}\sqrt{1+\frac{1}{4\tilde{n}^2}}[3(\varepsilon_k n_d\langle \hat{d}_k\hat{h}_{-k}\rangle - \varepsilon_0\eta\langle \hat{d}_k^\dagger \hat{d}_k\rangle) + 2\varepsilon_0\xi_d\langle \hat{d}_k\hat{h}_{-k}\rangle]\\ +3(\varepsilon_k n_d - \varepsilon_0\xi_d)\langle \hat{d}_k^\dagger \hat{d}_k\rangle + 3\varepsilon_0\eta^*\langle \hat{d}_k\hat{h}_{-k}\rangle\end{matrix}\right],
\end{aligned} \tag{A17}$$

with $\langle \hat{h}^\dagger_{-k}\hat{h}_{-k}\rangle = \langle \hat{d}_k^\dagger \hat{d}_k\rangle$. We integrate these equations to get the results in the main paper.

[1] J. P. Sethna, *Statistical Mechanics: Entropy, Order Parameters, and Complexity* (Oxford University Press, Oxford, New York, 2006).
[2] S. L. Sondhi, S. M. Girvin, J. P. Carini, and D. Shahar, Rev. Mod. Phys. **69**, 315 (1997).

[3] H. Aoki, N. Tsuji, M. Eckstein, M. Kollar, T. Oka, and P. Werner, Rev. Mod. Phys. **86**, 779 (2014).
[4] C. Orzel, A. K. Tuchman, M. L. Fenselau, M. Yasuda, and M. A. Kasevich, Science **291**, 2386 (2001).
[5] M. Greiner, O. Mandel, and T. Esslinger, Nature (London) **415**, 39 (2002).
[6] T. Stöferle, H. Moritz, C. Schori, M. Köhl, and T. Esslinger, Phys. Rev. Lett. **92**, 130403 (2004).
[7] C. L. Hung, X. Zhang, N. Gemelke, and C. Chin, Phys. Rev. Lett. **104**, 160403 (2010).
[8] D. Chen, M. White, C. Borries, and B. De Marco, Phys. Rev. Lett. **106**, 235304 (2011).
[9] S. Braun, M. Friesdorf, S. S. Hodgman, M. Schreiber, J. P. Ronzheimer, A. Riera, M. del Rey, I. Bloch, J. Eisert, and U. Schneider, Proc. Natl. Acad. Sci. USA **112**, 3641 (2014).
[10] M. P. A. Fisher, P. B. Weichman, G. Grinstein, and D. S. Fisher, Phys. Rev. B **40**, 546 (1989).
[11] P. Barmettler, D. Poletti, M. Cheneau, and C. Kollath, Phys. Rev. A **85**, 053625 (2012).
[12] K. Sheshadri, H. R. Krishnamurthy, R. Pandit, and T. V. Ramaktishnan, Europhys. Lett. **22**, 257 (1993).
[13] D. Jaksch, C. Bruder, J. I. Cirac, C. W. Gardiner, and P. Zoller, Phys. Rev. Lett. **81**, 3108 (1998).
[14] H. Tasaki, J. Phys.: Condens. Matter **10**, 4353 (1998).
[15] V. Gurarie, L. Pollet, N. Prokof'ev, B. Svistunov, and M. Troyer, Phys. Rev. B **80**, 214519 (2009).
[16] M. Cheneau, P. Barmettler, D. Poletti, M. Endres, P. Schauss, T. Fukuhara, C. Gross, I. Bloch, C. Kollath, and S. Kuhr, Nature (London) **481**, 484 (2012).
[17] S. S. Natu, D. C. McKay, B. DeMarco, and E. J. Mueller, Phys. Rev. A **85**, 061601 (2012).
[18] A. Griffin, Phys. Rev. B **53**, 9341 (1996).
[19] A. Polkovnikov, K. Sengupta, A. Silva, and M. Vengalattore, Rev. Mod. Phys. **83**, 863 (2011).
[20] J. Dziarmaga, Adv. Phys. **59**, 1063 (2010).
[21] W. Zwerger, J. Opt. B: Quantum Semiclassical Opt. **5**, S9 (2003).
[22] J. Zakrzewski, Phys. Rev. A **71**, 043601 (2005).
[23] F. M. Cucchietti, B. Damski, J. Dziarmaga, and W. H. Zurek, Phys. Rev. A **75**, 023603 (2007).
[24] L. Amico and V. Penna, Phys. Rev. Lett. **80**, 2189 (1998).
[25] A. Polkovnikov, Phys. Rev. B **72**, 161201 (2005).
[26] P. Navez and R. Schützhold, Phys. Rev. A **82**, 063603 (2010).
[27] M. Tylutki, J. Dziarmaga, and W. H. Zurek, J. Phys.: Conf. Ser. **414**, 012029 (2013).
[28] V. A. Kashurnikov, N. Prokof'ev, and B. Svistunov, Phys. Rev. A **66**, 031601 (2002).
[29] C. Kollath, A. M. Läuchli, and E. Altman, Phys. Rev. Lett. **98**, 180601 (2007).
[30] J. D. Sau, B. Wang, and S. Das Sarma, Phys. Rev. A **85**, 013644 (2012).
[31] A. Polkovnikov, S. Sachdev, and S. M. Girvin, Phys. Rev. A **66**, 053607 (2002).
[32] A. K. Tuchman, C. Orzel, A. Polkovnikov, and M. A. Kasevich, Phys. Rev. A **74**, 051601 (2006).
[33] D. Boyanovsky and H. J. de Vega, Phys. Rev. D **47**, 2343 (1993).
[34] K. Sengupta and N. Dupuis, Phys. Rev. A **71**, 033629 (2005).
[35] M. P. Kennett and D. Dalidovich, Phys. Rev. A **84**, 033620 (2011).
[36] J. Hubbard, Proc. R. Soc. London, Ser. A **276**, 238 (1963).
[37] I. Bloch and W. Zwerger, Rev. Mod. Phys. **80**, 885 (2008).
[38] J. K. Freericks and H. Monien, Europhys. Lett. **26**, 545 (1994).
[39] T. D. Kühner and H. Monien, Phys. Rev. B **58**, R14741(R) (1998).
[40] N. Elstner and H. Monien, Phys. Rev. B **59**, 12184 (1999).
[41] B. Capogrosso-Sansone, N. Prokof'ev, and B. Svistunov, Phys. Rev. B **75**, 134302 (2007).
[42] B. Capogrosso-Sansone, Ş. G. Söyler, N. Prokof'ev, and B. Svistunov, Phys. Rev. A **77**, 015602 (2008).
[43] N. Teichmann, D. Hinrichs, M. Holthaus, and A. Eckardt, Phys. Rev. B **79**, 100503(R) (2009).
[44] J. Schachenmayer, L. Pollet, M. Troyer, and A. J. Daley, Phys. Rev. A **89**, 011601 (2014).
[45] Z. Cai and T. Barthel, Phys. Rev. Lett. **111**, 150403 (2013).
[46] D. Poletti, P. Barmettler, A. Georges, and C. Kollath, Phys. Rev. Lett. **111**, 195301 (2013).
[47] H. Pichler, J. Schachenmayer, A. J. Daley, and P. Zoller, Phys. Rev. A **87**, 033606 (2013).
[48] D. Poletti, J.-S. Bernier, A. Georges, and C. Kollath, Phys. Rev. Lett. **109**, 045302 (2012).
[49] H. Pichler, A. J. Daley, and P. Zoller, Phys. Rev. A **82**, 063605 (2010).
[50] Y. Yanay and E. J. Mueller, Phys. Rev. A **90**, 023611 (2014).